Intramolecular Electron Transfer in Linked Tris(2,2′-bipyridine)ruthenium(II)/Diquat Complexes

Laura F. Cooley, Christine E. L. Headford, C. Michael Elliott,* and David F. Kelley*,†

Contribution from the Department of Chemistry, Colorado State University, Fort Collins, Colorado 80523. *Received February 16, 1988*

Abstract: Electron transfer (ET) rates have been measured for a series of linked tris(2,2′-bipyridine)ruthenium(II)/diquat complexes in room-temperature acetonitrile solutions, using time-resolved picosecond emission and absorption spectroscopies. The rate of ET from the metal-to-ligand charge transfer (MLCT) states to the diquat acceptor has been analyzed in terms of a simple kinetic model, in which MLCT exciton hopping is fast, ET to the diquat is rate limiting, and the latter occurs only from MLCT states localized on bipyridine ligands which are linked to diquat acceptors. Electrochemical data for Ru 2+/1+ and Ru 1+/0 reduction potentials have been related to MLCT state energies and used in the model. Semiquantitative agreement was found between the model's predictions and measured ET times. A linear relationship was found to exist between ET driving force and the log of the ET rate. Reverse (diquat to ruthenium) ET rates were determined to be fast relative to forward rates.

I. Introduction

Recent studies of excited-state electron transfer in the ruthenium tris(bipyridine) family of complexes have shown that these compounds, in conjunction with electron acceptors, hold promise in terms of their ability to convert optical energy.[1-8] Most charge separation systems are based on intermolecular electron transfer. Similar intramolecular electron transfer can also be achieved.[9-12] The design and synthesis of metal complexes which undergo intramolecular electron transfer, from $d\pi-\pi^*$ metal-to-ligand charge transfer (MLCT) states to linked electron acceptors, have been successful, and it has been found that modifications in the structure of these acceptors alter their reduction potentials in well-understood ways.[9] In addition, cyclic voltammetric measurements of ligand reduction potentials (nominally Ru 2+/1+) have revealed how subtle modification (e.g., methyl substitution) of one or more bipyridine rings of a ruthenium tris(bipyridine) complex, $Ru(bpy)_3^{2+}$, alters its lowest π^* energy.[13-15] Since the electron transfer (ET) event under study constitutes moving an electron from the lowest π^* level of the complex to a linked electron acceptor, understanding how changes in π^* energy and electron acceptor reduction potential affect the ET rate must precede the ability to develop and, ultimately, control the energy conversion process.

It is well known that $Ru(bpy)_3^{2+}$ and its alkyl-substituted derivatives have a long-lived (300–600 ns) luminescence, due to emission from ^{3}MLCT states.[14,16,17] When an *N,N*′-diquaternary-2,2′-bipyridinium salt (diquat) is intramolecularly linked to a ligand of the complex, however, MLCT emission is quenched by electron transfer to the diquat acceptor.[9] In this paper, we present electrochemical and time-resolved (picosecond) spectroscopic data, revealing ET rates for a series of substituted mixed-ligand ruthenium tris(bipyridine) complexes, linked to diquat acceptors by a methylene chain. The particular complexes studied differ in diquat reduction potential and MLCT state energies.

It is well established that, for $Ru(bpy)_3^{2+}$ in solution, MLCT excitation is rapidly localized on a single bipyridine ligand.[18-23] Our results show that the rate of luminescence quenching (forward ET) in diquat-linked complexes depends, systematically, on both the diquat reduction potential and on the difference in energy between the two types of MLCT states of a given complex, i.e., MLCT states localized on ligands linked to a diquat, and those localized on the other ligands. These two types of ligands and their corresponding MLCT states will hereafter be referred to as "adjacent" and "remote", respectively, according to their proximity to the diquat acceptor. We anticipate that ET from adjacent and remote ligands may have very different rates. Determination of the rate of bipyridine exciton hopping (ligand-to-ligand ET) is also crucial for understanding the overall ET mechanism. Limits on these rates will be inferred from the data presented here.

The general form of the complexes studied may be written as $Ru^{II}(4mn\text{-}DQ^{2+})_N(L)_{3-N}$, where N is 1, 2, or 3. The ligands, L, refer to either a bipyridine (bpy), a dimethylated bipyridine (4,4′-Me_2bpy) ≡ DMB), or a tetramethylated bipyridine (4,4′,5,5′-Me_4bpy ≡ TMB). The ligand $4mn\text{-}DQ^{2+}$ (structure given below) indicates a bipyridine which is methylated in the

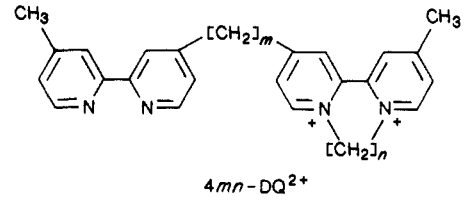

$4mn\text{-}DQ^{2+}$

4-position, linked at the 4′-position, via a methylene chain of length m, to a diquat. The nitrogens of the diquat are connected by a

† Alfred P. Sloan Fellow.

(1) Creutz, C.; Sutin, N. *Proc. Nat. Acad. Sci. U.S.A.* **1975**, *72*, 2858–2862.
(2) Young, R. C.; Meyer, T. J.; Whitten, D. G. *J. Am. Chem. Soc.* **1975**, *97*, 4781–4782.
(3) Lin, C.-T.; Sutin, N. *J. Phys. Chem.* **1975**, *80*, 97–105.
(4) Kalyanasundaram, K. *Coord. Chem. Rev.* **1982**, *46*, 159–244.
(5) Sutin, N.; Creutz, C. *Pure Appl. Chem.* **1980**, *52*, 2717–2738.
(6) Whitten, D. G. *Acc. Chem. Res.* **1980**, *13*, 83–90.
(7) Meyer, T. J. *Acc. Chem. Res.* **1978**, *11*, 94–100.
(8) Balzani, V.; Moggi, L.; Manfrin, M. F.; Bolletta, F.; Gleria, M. *Science* **1975**, *189*, 852–856.
(9) Elliott, C. M.; Freitag, R. A.; Blaney, D. D. *J. Am. Chem. Soc.* **1985**, *107*, 4647–4655.
(10) Elliott, C. M.; Freitag, R. A. *J. Chem. Soc., Chem. Commun.* **1985**, 156–157.
(11) Westmoreland, T. D.; Le Bozec, H.; Murray, R. W.; Meyer, T. J. *J. Am. Chem. Soc.* **1983**, *105*, 5952–5954.
(12) Matsuo, T.; Skamoto, T.; Takuma, K.; Sakura, K.; Ohsako, T. *J. Phys. Chem.* **1981**, *85*, 1277–1279.
(13) Ferguson, J.; Mau, A. W. H.; Sasse, W. H. F. *Chem. Phys. Lett.* **1979**, *68*, 21–24.
(14) McClanahan, S. F.; Dallinger, R. F.; Holler, F. J.; Kincaid, J. R. *J. Am. Chem. Soc.* **1985**, *107*, 4853–4860.
(15) Mabrouk, P. A.; Wrighton, M. S. *Inorg. Chem.* **1986**, *25*, 526–531.
(16) Lin, C.-T.; Bottcher, W.; Chou, M.; Creutz, C.; Sutin, N. *J. Am. Chem. Soc.* **1976**, *98*, 6536–6544.
(17) Navon, G.; Sutin, N. *Inorg. Chem.* **1974**, *13*, 2159–2164.
(18) Bradley, P. G.; Kress, N.; Hornberger, B. A.; Dallinger, R. F.; Woodruff, W. H. *J. Am. Chem. Soc.* **1981**, *103*, 7441–7446.
(19) Dallinger, R. F.; Woodruff, W. H. *J. Am. Chem. Soc.* **1979**, *101*, 4391–4393.
(20) Motten, A. G.; Hanck, K. W.; DeArmond, M. K. *J. Am. Chem. Soc.* **1981**, *79*, 541–546.
(21) Morris, D. E.; Hanck, K. W.; DeArmond, M. K. *J. Am. Chem. Soc.* **1983**, *105*, 3032–3038.
(22) Elliott, C. M.; Hershenhart, E. J. *J. Am. Chem. Soc.* **1982**, *104*, 7519–7526.
(23) Heath, G. A.; Yellowlees, C. J.; Braterman, P. S. *J. Chem. Soc., Chem. Commun.* **1981**, 287–289.

0002-7863/88/1510-6673$01.50/0

chain of methylene groups of length n. In the present work, unless otherwise noted, m equals 2, and n is either 2, 3, or 4. Thus, we will speak of 422-DQ^{2+}, 423-DQ^{2+}, and 424-DQ^{2+} ligands.

Variation in the reduction potential of the diquat electron acceptor may be accomplished by changing the number, n, of methylene units in the bridge linking the pyridine nitrogens.[9] The smaller n, the easier the diquat is to reduce. Variation in the energy difference between adjacent and remote MLCT states of a given complex was accomplished by changing the number of methyl groups on the remote ligands.

II. Experimental Section

Materials. Unless otherwise specified, all solvents and chemicals were reagent grade and used without purification. 2,2′-Bipyridine (bpy), ethylene glycol, 1,4-dibromobutane, and *o*-dichlorobenzene were supplied by Aldrich. 4,4′-Dimethyl-2,2′-bipyridine (DMB) was obtained from Reilly Tar and Chemical, Indianapolis, IN, and was recrystallized from ethyl acetate several times before use. Diethyl ether was obtained from Mallinckrodt and acetonitrile from J. T. Baker. NH_4PF_6 was obtained from Ozark-Mahoning Pennwalt, and KNO_3 from Mallinckrodt.

Preparation of Linked Bipyridine–Diquat Ligands. Typically, the linked bipyridine–diquat ligands were checked for purity by NMR, electrochemistry, and TLC prior to their use for the preparation of the various ruthenium complexes described below.

Preparation of (422-DQ^{2+})(PF_6^-)$_2$ and (453-DQ^{2+})(PF_6^-)$_2$ ligands was reported previously in ref 9.

(424-DQ^{2+})(PF_6^-)$_2$. 1,2-Bis[4-(4′-methyl-2,2′-bipyridyl)]ethane[9] (dimer 1) (0.25 g) was added to 1 mL of *o*-dichlorobenzene in a glass tube, followed by addition of 1,4-dibromobutane (85 μL) and 3.5 mL of *o*-dichlorobenzene. The reaction mixture was degassed by three freeze–pump–thaw cycles and sealed under vacuum. After thawing, the sealed sample was placed in a tube furnace at 140 °C and heated for 3 days. The resulting pink-colored solid was filtered and washed with 10 mL of diethyl ether. The intermediate product (424-DQ^{2+})(Br^-)$_2$ was dried at room temperature under vacuum overnight. Using 15 mL of distilled water, the product was washed through a medium porosity frit to remove insoluble unreacted dimer 1, yielding an orange-colored solution. A solution of 2 g of NH_4PF_6 in 5 mL of distilled water was filtered into the above orange solution, yielding the crude solid product as the PF_6^- salt, which was isolated by centrifugation. The product was purified by medium-pressure liquid chromatography (MPLC) on water-washed, grade 62, 60–200 mesh silica gel, eluting with 5:4:1 acetonitrile–distilled water–saturated aqueous KNO_3. The presence of the product in the eluent was detected using an ISCO single-wavelength UV detector operated with a 280–310-nm band-pass. The fraction containing the 424-DQ^{2+} product was collected and reduced to about one-third its original volume by rotary evaporation to remove all of the acetonitrile, and a filtered solution containing 2 g of NH_4PF_6 in 5 mL of distilled water was added. The product, as the PF_6^- salt, came out of solution as a light pink/white flocculent precipitate. The purified product was again isolated by centrifugation, washed several times with distilled water, and dried under vacuum at room temperature overnight.

(453-DQ^{2+})(PF_6^-)$_2$. This compound was prepared according to the literature procedure for the synthesis of (423-DQ^{2+})(PF_6^-)$_2$,[9] except that 1,5-bis[4-(4′-methyl-2,2′-bipyridyl)]pentane[24] (dimer 2) was employed, rather than dimer 1, as the starting material.

Preparation of Tris(bipyridine)ruthenium(II) Complexes. All complexes having linked diquat-type ligands were prepared under red lights. Reaction flasks and chromatography columns were protected from light and covered with Al foil. Purity was typically verified by TLC, cyclic voltammetry, and NMR.

Preparation of the complexes Ru(bpy)$_2$(423-DQ^{2+})(PF_6^-)$_4$, Ru(bpy)$_2$(422-DQ^{2+})(PF_6^-)$_4$, Ru(DMB)$_2$(423-DQ^{2+})(PF_6^-)$_4$, Ru(TMB)$_2$(423-DQ^{2+})(PF_6^-)$_4$, and Ru(423-DQ^{2+})$_3$(PF_6^-)$_8$ has been previously reported in ref 9.

Ru(bpy)$_2$(424-DQ^{2+})(PF_6^-)$_4$. Ru(bpy)$_2$Cl$_2$[25] (0.068 g) in 70 mL of ethylene glycol was stirred under N_2 purge for 10 min. The mixture was then heated for 1 h at ca. 175 °C. After the mixture was cooled to room temperature, 100 mg (1 equiv) of (424-DQ^{2+})(PF_6^-)$_2$ was added to the solution and the reaction mixture heated to 120 °C for 30 min. After cooling again to room temperature, the solution was diluted with distilled water (2:1) and a filtered solution of NH_4PF_6 (3.0 g in 10 mL of distilled water) was added. The resulting orange-yellow precipitate was isolated by centrifugation, washed with distilled water, and dried under vacuum at room temperature. MPLC on water-washed, grade 62 silica gel was used for purification; the eluent was the same as that used for (424-DQ^{2+})(PF_6^-)$_2$ given above. Acetonitrile was removed by rotary evaporation from those fractions of the eluent containing the desired product (as determined by TLC). A filtered solution of NH_4PF_6 (3 g in 10 mL of distilled water) was added to the solution, resulting in precipitation of the orange product, which was isolated by centrifugation. The solid was washed with distilled water and dried under vacuum at room temperature overnight.

Ru(bpy)$_2$(453-DQ^{2+})(PF_6^-)$_4$. This compound was prepared, isolated, and purified by a method analogous to that of Ru(bpy)$_2$(424-DQ^{2+})(PF_6^-)$_4$, given above, but employing (453-DQ^{2+})(PF_6^-)$_2$.

Ru(DMB)(423-DQ^{2+})$_2$(PF_6^-)$_6$. A mixture of Ru(DMSO)$_4$Cl$_2$[26] (0.019 g), DMB (0.008 g, 1 equiv), and (423-DQ^{2+})(PF_6^-)$_2$ (0.06 g, 2 equiv) in 10 mL of ethylene glycol was stirred under N_2 while the reaction flask was slowly heated to 125 °C and held there for 10 min. After cooling to room temperature in a cold water bath, the reaction solution was diluted with 10 mL of distilled water and the crude product precipitated by addition of an NH_4PF_6 solution. The crude product consisted of a mixture of tris(bipyridine) complexes having different numbers of diquat-containing bipyridines per ruthenium. Isolation and purification of the desired product were accomplished by chromatography on silica gel as described above. The various complexes with different numbers of diquat units separated completely under these conditions. Acetonitrile was removed from the fraction containing the desired product by rotary evaporation, and the complex precipitated by addition of NH_4PF_6. Isolation was accomplished as described above. The orange-red solid was identified as the desired product and its purity verified by cyclic voltammetry.

Ru(bpy)(423-DQ^{2+})$_2$(PF_6^-)$_6$. A mixture of Ru(bpy)Cl$_4$[27] (0.005 g) and (423-DQ^{2+})(PF_6^-)$_2$ (0.021 g, 2.3 equiv) in 5 mL of ethylene glycol was stirred under N_2 and heated to 120 °C for 10 min. The reaction mixture was cooled to room temperature and diluted 2:1 with distilled water; the product was precipitated with NH_4PF_6. Purification and isolation of the orange-yellow product was accomplished in the manner previously described for Ru(bpy)$_2$(424-DQ^{2+})(PF_6^-)$_4$.

Ru(bpy)$_3$(PF_6^-)$_2$. Ru(DMSO)$_4$Cl$_2$[26] (0.02 g) and bpy (0.02 g, 3.1 equiv) were combined in 10 mL of ethylene glycol. The mixture was heated quickly to near reflux. After cooling to room temperature, the solution was diluted 3:1 with distilled water. To this solution, sufficient aqueous NH_4PF_6 was added to precipitate all of the complex and render the solution colorless. The solid was filtered on a glass frit, rinsed with several portions of distilled water, and dried at room temperature under vacuum.

Ru(DMB)$_3$(PF_6^-)$_2$. Preparation of this complex was analogous to that of Ru(bpy)$_3$(PF_6^-)$_2$, given above, with DMB used instead of bpy.

Ru(bpy)$_2$(DMB)(PF_6^-)$_2$. Ru(bpy)$_2$Cl$_2$[25] (0.02 g) was added to 15 mL of ethylene glycol and the solution heated to between 120 and 140 °C. The reaction solution turned from purple to cherry red. To this solution, DMB (0.01 g, 1.5 equiv) was added and heating continued for 30 min. After cooling, the complex was isolated as the PF_6^- salt in the same manner as for Ru(bpy)$_3$(PF_6^-)$_2$, above.

Cyclic Voltammetry (CV). The equipment and cells for cyclic voltammetry have been described elsewhere.[28] All voltammograms were run in acetonitrile (Burdick & Jackson "Distilled in Glass") with 0.10 M tetrabutylammonium hexafluorophosphate (TBAPF$_6$) as supporting electrolyte, at a glassy carbon electrode. All potentials were measured relative to SCE.

Preparation of Samples for Kinetic Studies. Solid samples of all the complexes containing diquat ligands were stored in a drybox (Vacuum Atmospheres Corp.) under N_2 atmosphere and wrapped in Al foil to prevent photodecomposition in the presence of O_2. Solution samples of the complexes in acetonitrile (J.T. Baker, Photrex Reagent, purged with N_2) were prepared, transferred to sample cells, and sealed under N_2 all in the drybox. Sample volumes were 1–2 mL and typical concentrations were ca. 10^{-3} M. Sample cells consisted of a rectangular Pyrex tube (2 × 4 mm i.d.; 1-mm wall) sealed on one end and attached to a Kontes Teflon-and-glass valve on the other end. Laser excitation was through the flat face of the cells, path length 2 mm. When not in use, sealed samples were stored in a refrigerator and covered with Al foil.

Picosecond Kinetics. The apparatus used for time-resolved emission and absorption measurements have been described in detail previously.[29,30] Briefly, both are based on an active/passive mode-locked Nd:

(24) Schmehl, R. H.; Auerbach, R. A.; Wacholtz, W. F.; Elliott, C. M.; Freitag, R. A. *Inorg. Chem.* **1986**, *25*, 2440–2445.
(25) Sullivan, B. P.; Salmon, D. J.; Meyer, T. J. *Inorg. Chem.* **1978**, *17*, 3334–3341.
(26) Evans, I. P.; Spencer, A.; Wilkinson, G. *J. Chem. Soc., Dalton Trans.* **1973**, 204–209.
(27) Dwyer, F. P.; Goodwin, H. A.; Gyarfas, E. C. *Aust. J. Chem.* **1963**, *16*, 42–50.
(28) Elliott, C. M.; Hershenhart, E.; Finke, R. G.; Smith, B. L. *J. Am. Chem. Soc.* **1981**, *103*, 5558–5566.

Table I. Reduction Potentials for Ruthenium Complexes.

complex	$E_{1/2}$ in CH_3CN vs. SCE					
	Ru 3+/2+	DQ^{2+} 2+/1+	DQ^{2+} 1+/0	Ru 2+/1+	Ru 1+/0	Ru 0/1−
$[Ru(bpy)_3][PF_6]_2$	+1.28			−1.34	−1.53	−1.78
$[Ru(DMB)_3][PF_6]_2$	+1.15			−1.46	−1.64	−1.86
$[Ru(TMB)_3][PF_6]_2$	+1.01			−1.63	−1.82	−2.07
$[Ru(bpy)_2(DMB)][PF_6]_2$	+1.22			−1.37	−1.57	−1.82
$[Ru(bpy)_2(423\text{-}DQ^{2+})][PF_6]_4$	+1.24	−0.64	−0.92	−1.36	−1.56	−1.81
$[Ru(DMB)_2(423\text{-}DQ^{2+})][PF_6]_4$	+1.13	−0.65	−0.93	−1.45	−1.64	−1.87
$[Ru(TMB)_2(423\text{-}DQ^{2+})][PF_6]_4$	+1.06	−0.65	−0.93	−1.51	−1.79	−2.03
$[Ru(bpy)(423\text{-}DQ^{2+})_2][PF_6]_6$	+1.19	−0.65	−0.93	−1.40	−1.62	−1.86
$[Ru(DMB)(423\text{-}DQ^{2+})_2][PF_6]_6$	+1.12	−0.66	−0.94	−1.46	−1.64	−1.88
$[Ru(423\text{-}DQ^{2+})_3][PF_6]_8$	+1.15	−0.65	−0.93	−1.45	−1.64	−1.88
$[Ru(bpy)_2(422\text{-}DQ^{2+})][PF_6]_4$	+1.25	−0.44	−0.89	−1.35	−1.56	−1.81
$[Ru(bpy)_2(424\text{-}DQ^{2+}][PF_6]_4$	+1.23	−0.77	−0.90	−1.37	−1.57	−1.83

YAG laser. For both studies, samples were excited with the third harmonic, 355-nm light (30 ps, 0.15 mJ) pulses focused to a ca. 1-mm spot size. Detection of transient emission was accomplished with a Hamamatsu C979 streak camera, coupled to a PAR 1254E SIT Vidicon and interfaced to a DEC LSI 11/02 computer. The temporal instrument response was ca. 25 ps for the fastest streak speed, and 180 ps for the slowest. In all cases, a Hoya Glass R-62 filter was placed before the streak camera to permit detection at wavelengths greater than 620 nm.

For absorption, the pump pulse was provided by 355-nm light, as above. To probe the sample, emission from a solution of ca. 1×10^{-5} M of the organic dye Coumarin 460 in ethylene glycol was used. The dye fluorescence was spacially filtered, collimated, and focused through the sample excitation volume. The light was then recollimated and focused into the streak camera described above. Since a transient absorption in the sample alters the apparent kinetics of dye emission as viewed by the streak camera, comparison of dye emission with and without sample excitation yields accurate absorption kinetics. An interference filter (450 ± 25 nm) was placed before the streak camera, allowing for measurement of transient absorption in this wavelength range.

Emission decay and bleach recovery curves were fitted to single exponentials convolved with an instrument response function appropriate to the streak speed of the measurement.

III. Results

Electrochemical reduction potentials for the substituted ruthenium trisbipyridine complexes studied are listed in Table I. The table includes potentials for some complexes with, and some without, linked diquat electron acceptors. Data for the latter set of complexes are included since these reduction potentials will be needed in the Discussion.

Picosecond optical absorption and emission kinetic data were obtained. Emission decay curves were measured at wavelengths greater than 620 nm, following excitation at 355 nm. These measurements were made in room-temperature acetonitrile. Transitions to metal-centered d–d states and to ligand-localized $\pi-\pi^*$ states[23,31-33] result in absorption, at this wavelength, and both types of states are initially populated. Since a fast MLCT emission risetime is observed, we conclude that energy relaxation to MLCT states proceeds rapidly (<10 ps). When an electron acceptor is not present, luminescence from this state is long-lived, whereas in the presence of an electron acceptor such as diquat, the luminescence is rapidly quenched by electron transfer. The electron transfer time is therefore very nearly equal to the observed emission lifetime.

The onset of MLCT emission is at ca. 550–570 nm, with a maximum at 600–640 nm. When a filter allowing detection of emission >550 nm was used, a slight fast component was present in the emission decays. Further investigation showed that this fast component, presumably due to trace impurities, had a maximum at ca. 500 nm, and is therefore unrelated to MLCT emission. When a >620-nm filter was used, there was no evidence of a fast component. Observing at these wavelengths thus ensures that the kinetics obtained are due only to MLCT emission. Figure 1 shows the emission decay curve obtained for $Ru(TMB)_2(423\text{-}DQ^{2+})$. Shown with it is the best fit of a single exponential to the data, with a decay time of 90 ps. Table II lists emission decay times for all the complexes studied.

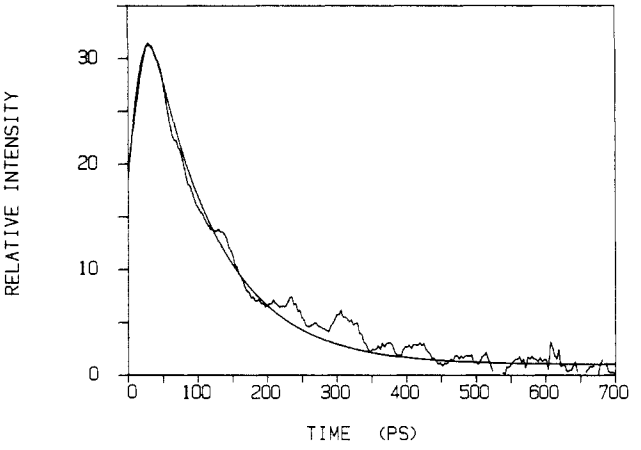

Figure 1. Emission decay curve obtained for $Ru(TMB)_2(423\text{-}DQ^{2+})$ in acetonitrile at room temperature, observing at λ >620 nm. Shown with the experimental curve is its best fit to a single exponential (decay time 90 ps).

Table II. Observed Emission Decay and Bleach Recovery Times (k_f^{-1}).

complex	absorption bleach recovery times (ps)	emission decay times (ps)
$(Ru(bpy)_2(423\text{-}DQ^{2+}))^{4+}$	1700	1700
$(Ru(DMB)_2(423\text{-}DQ^{2+}))^{4+}$	180	150
$(Ru(TMB)_2(423\text{-}DQ^{2+}))^{4+}$	80	90
$(Ru(bpy)(423\text{-}DQ^{2+})_2)^{6+}$	450	450
$(Ru(DMB)(423\text{-}DQ^{2+})_2)^{6+}$	—	125
$(Ru(423\text{-}DQ^{2+})_3)^{8+}$	170	150
$(Ru(bpy)_2(422\text{-}DQ^{2+}))^{4+}$	250	290
$(Ru(bpy)_2(424\text{-}DQ^{2+}))^{4+}$	6100	6500

Picosecond kinetics were also obtained for repopulation of the ground state following excitation at 355 nm. Excitation of the complex results in a reduced absorbance or bleach at ca. 450 nm, corresponding to the MLCT absorption. Recovery of this bleach depends on both the rate of MLCT state decay (forward ET) and the rate of reverse ET. Bleach recovery curves at 450 ± 25 nm have therefore been obtained in order to deduce estimates of reverse ET times. Figure 2 shows the bleach recovery curve obtained for $Ru(bpy)_2(423\text{-}DQ^{2+})$ and its corresponding best fit to a single exponential (1700 ps). Table II lists bleach recovery times for the complexes studied. In all cases, the emission decay and bleach recovery times for a given complex are the same, within experimental error. Since better signal-to-noise ratios were obtained for absorption spectra, bleach recovery times will, where possible, be used for forward ET times in the Discussion.

(29) Brucker, G. A.; Kelley, D. F. *J. Phys. Chem.* **1987**, *91*, 2856–2861.
(30) Jang, D.-J.; Kelley, D. F. *Rev. Sci. Instrum.* **1985**, *56*, 2205–2208.
(31) Lytle, F. E.; Hercules, D. M. *J. Am. Chem. Soc.* **1969**, *91*, 6384–6386.
(32) Bryant, G.; Ferguson, J. E.; Powell, H. *Aust. J. Chem.* **1971**, *24*, 257–273.
(33) Felix, E.; Ferguson, J.; Gudel, H. V.; Ludi, A. *J. Am. Chem. Soc.* **1980**, *102*, 4096–4102.

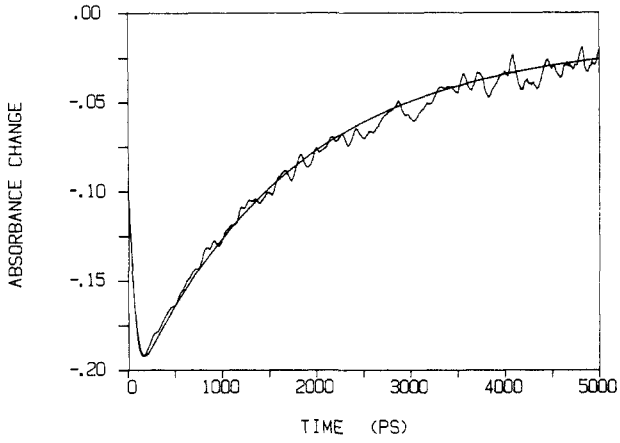

Figure 2. Bleach recovery curve (absorption) obtained for $Ru(bpy)_2$-(423-DQ^{2+}) in acetonitrile at room temperature, observing at 450 ± 25 nm. Also shown is the best fit of a single exponential to this curve, with a bleach recovery time of 1700 ps.

Scheme I

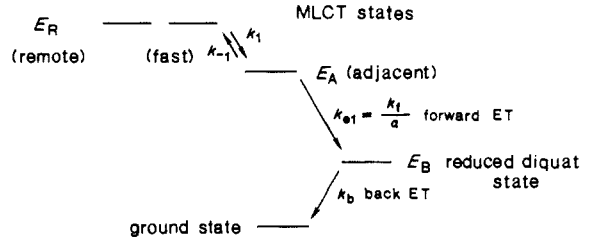

IV. Discussion

Proposed ET Scheme. The decay times and reduction potentials presented in the previous section may be analyzed in the framework of Scheme I. In this scheme, E_A and E_R refer respectively to the energies of MLCT states localized on the adjacent and remote ligands of the diquat-linked complexes. The reduced diquat state is indicated with energy E_B.

Two basic ideas are postulated in this model: first, that forward electron transfer, indicated by the rate constant k_f, occurs only from MLCT states localized on ligands adjacent to the diquat. Electron transfer from a remote ligand is thus assumed to be much slower than that from an adjacent ligand, owing to its longer electron-transfer distance.[34,35]

Second, the model postulates the existence of a rapidly established thermal equilibrium between remote and adjacent MLCT state populations. Although no direct experimental evidence of a fast equilibrium appears to be available from the literature, the results of time-resolved resonance Raman studies of McClanahan et al.[14] find that for excited $Ru(bpy)_2(DMB)^{2+}$, the unpaired electron is localized on bpy to a larger extent than on a DMB ligand. In excited $Ru(bpy)(DMB)_2^{2+}$ the same is true, but to a lesser extent than for $Ru(bpy)_2(DMB)^{2+}$. Since these spectra were taken on the 10-ns timescale, their results do not permit determination of whether or not the equilibrium is established faster than this limit.

The ordering of adjacent and remote MLCT state energies indicated in Scheme I depends on the degree of methyl substitution in the complex. In general, the presence of electron-donating methyl or methylene substituents raises (LUMO) bipyridine π^* energies,[14,15] and correlates with more negative values of the Ru 2+/1+ reduction potential.[36] Since the Ru 2+/1+ reduction is largely ligand-centered, and best described as $Ru^{II}L_3 + e^- \rightarrow Ru^{II}L^{-}\cdot L_2$, the reduced ligand is a radical anion and is destabilized by alkyl substitution. The difference in energy between adjacent and remote MLCT states, $E_A - E_R$, will hereafter be referred to as E_{AR}. This quantity may be estimated from Ru 2+/1+ and Ru 1+/0 reduction potentials and is evaluated in the Energetics section, below.

Based on Scheme I, the following equations may be written for the time dependence of the total MLCT state population, M, the reduced diquat population, B, and the change in ground-state population, G. M is equal to $A + R$, where A and R are the adjacent and remote MLCT populations, respectively.

$$-dM/dt = k_f M = k_{et} A = k_{et}\alpha M \qquad (\alpha = A/M;\ k_f = \alpha k_{et})$$

$$dB/dt = k_f M - k_b B$$

$$dG/dt = k_b B$$

These equations are valid only in the limit where the rate of equilibration between adjacent and remote MLCT states is fast relative to the rate of electron transfer from the adjacent MLCT state to diquat. (Thus, it is assumed that $k_1 + k_{-1} \gg k_{et}$). The apparent emission decay rate constant is given by k_f in this model. Solving the above equations yields:

$$M(t) = M_0 e^{-k_f t} = M_0 e^{-\alpha k_{et} t} \tag{1}$$

$$B(t) = \frac{M_0 k_f}{k_f - k_b}(e^{-k_f t} - e^{-k_b t}) \tag{2}$$

$$G(t) = -M(t) - B(t) = \frac{M_0}{k_b - k_f}[-k_f e^{-k_b t} + 2k_f e^{-k_f t} - k_b e^{-k_f t}] \tag{3}$$

where M_0 is the initial, total MLCT state population, and α is the fraction of MLCT population localized on adjacent ligands.

Forward Electron Transfer. Equation 1, for the time dependence of the total population of MLCT states (adjacent plus remote), describes a single exponential decay curve with decay rate, k_f. According to the model above, this apparent electron transfer rate is equal to the product of the "adjacent" electron transfer rate, k_{et}, and α, the fraction of MLCT population localized on the adjacent ligand(s). Since $K_{eq} = A/R$, α is given by

$$\alpha = K_{eq}/(1 + K_{eq}) \tag{4}$$

where the equilibrium constant is given by the familiar expression,

$$K_{eq} = (n_A/n_R)e^{-E_{AR}/RT} \tag{5}$$

E_{AR}, as stated earlier, is the energy difference between MLCT states localized on the adjacent and remote ligands, and n_A and n_R are statistical factors equal to the number of adjacent and remote ligands, respectively. Once E_{AR} is known, K_{eq} and α may be determined. If all ligands were equivalent and linked to the same type of diquat acceptor, as is the case for $Ru(423\text{-}DQ^{2+})_3$, α would equal one, and the adjacent electron transfer rate would equal the apparent ET rate. In general, however, α will be less than unity. Evaluation of the above model requires determination of α and k_{et}, covered in later sections.

Reverse Electron Transfer. Repopulation of the ground state depends on both the forward (k_f) and back (k_b) electron transfer rates, as shown in eq 3. If $k_b \gg k_f$, $G(t)$ is a single exponential, approaching $M_0 \exp(-k_f t)$ in this limit, and the bleach recovery time would equal the emission decay time, k_f^{-1}. As this was found to be the case for all complexes where both times were measured, within experimental error (see Table II), it indicates that reverse ET is much faster than forward. From this observation, an upper limit may be placed on the reverse electron transfer time, if it is assumed that the rate of reverse ET is the same for all complexes with 423-type diquat acceptors. (This assumption is based on the fact that the diquat 2+/1+ reduction potential is more or less the same, within 20 mV, for all these complexes.) The shortest emission decay/bleach recovery time measured for any of the 423-type complexes was 80 ps, observed for $Ru(TMB)_2(423\text{-}DQ^{2+})$. As single exponential behavior was observed for bleach recovery, the actual reverse ET time is likely to be considerably less than this value. Based on simulations, a reverse ET time of

(34) Powers, M. J.; Salmon, D. J.; Callahan, R. W.; Meyer, T. J. *J. Am. Chem. Soc.* **1976**, *98*, 6731–6733.
(35) Marcus, R. A. *J. Chem. Phys.* **1956**, *24*, 966–978.
(36) Saji, T.; Aoyagui, S. *J. Electroanal. Chem. Interfacial Electrochem.* **1975**, *60*, 1–10.

Table III. Estimates of α and k_{et}

complex	E_{ar} (mV)	α	ΔG (mV)	k_{et}^{-1} (ps)	$(\alpha k_{et})^{-1}$ (ps)	k_f^{-1}(obsd) (ps)
$(Ru(bpy)_2(423\text{-}DQ^{2+}))^{4+}$	50 ± 10	0.064 ± 0.025	−360 ± 10	113 ± 10	1760 ± 800	1700
$(Ru(DMB)_2(423\text{-}DQ^{2+}))^{4+}$	0 ± 10	0.33 ± 0.1	−410 ± 10	70 ± 7	212 ± 90	180
$(Ru(TMB)_2(423\text{-}DQ^{2+}))^{4+}$	−100 ± 10	0.96 ± 0.02	−460 ± 10	43 ± 4	45 ± 5	80
$(Ru(bpy)(423\text{-}DQ^{2+})_2)^{6+}$	50 ± 10	0.21 ± 0.04	−370 ± 10	103 ± 11	490 ± 145	450
$(Ru(DMB)(423\text{-}DQ^{2+})_2)^{6+}$	0 ± 10	0.67 ± 0.09	−420 ± 10	63 ± 6	94 ± 20	125
$(Ru(423\text{-}DQ^{2+})_3)^{8+}$	0	1.0	−390 ± 10	85 ± 8	85 ± 8	170
$(Ru(bpy)_2(422\text{-}DQ^{2+}))^{4+}$	50 ± 10	0.064 ± 0.025	−570 ± 10	15 ± 3	235 ± 140	250
$(Ru(bpy)_2(424\text{-}DQ^{2+}))^{4+}$	50 ± 10	0.064 ± 0.025	−240 ± 10	358 ± 70	5600 ± 3000	6100

30 ps or more would be large enough to alter the bleach recovery kinetics, given by $G(t)$ combined with the 25-ps instrument response function, from a single exponential, and would therefore be detectable.

Energetics: Estimation of E_{AR} and α for Different Complexes. To estimate α, the fraction of MLCT states localized on adjacent ligands, values of the adjacent–remote MLCT energy splitting, E_{AR}, must be determined for each complex. E_{AR} may be estimated from Ru 2+/1+ and Ru 1+/0 reduction potentials, as is shown later in this section. The tacit assumption required for this procedure to be valid is that differences between remote and adjacent π^* energies do not vary with the charge on ruthenium. Although this charge essentially remains +2 for the ligand's first and second reductions, it is +3 in an actual MLCT state. This assumption surely introduces some error in the estimation of E_{AR}. However, the HOMO is of A_1 symmetry (D_3 point group approximation)[37] and removal of a single electron (MLCT excitation) is expected to affect each of the bipyridines about equally. It is therefore expected that electrochemical measurement can provide reasonable estimates of MLCT energy differences. Once an estimate of E_{AR} is made, eq 4 and 5 may then be used to solve for α in the various complexes.

In estimating E_{AR} values, π^* orbital energies associated with $42n\text{-}DQ^{2+}$ ligands will be treated as 4,4′-dimethylated bipyridine (DMB) ligands. This simplification is justified since ligands adjacent to diquat acceptors have a methyl group in the 4-position, and a diquat attached by a $-CH_2-CH_2-$ linkage to the 4′-position, and are thus similar to DMB ligands. Although this approximation also undoubtedly introduces some error, the reduction potentials given in Table I imply that the error is probably quite small, and DMB and $42n\text{-}DQ^{2+}$ ligands are thus expected to have the same π^* energies.

Determination of E_{AR} for all the complexes requires careful study of the Ru 2+/1+ and Ru 1+/0 potentials given in Table I. The Ru 2+/1+ potential corresponds to the easiest ligand-centered reduction, i.e., that placing an electron primarily on the ligand with the fewest methyl or methylene substituents. Placing a second electron in the complex corresponds to the next easiest ligand-centered reduction. In the case of $Ru(bpy)(423\text{-}DQ^{2+})_2$, for instance, the first electron reduces bpy, and the second reduces the methylated bipyridine of a $423\text{-}DQ^{2+}$ ligand. Values in the Ru 2+/1+ and Ru 1+/0 columns of Table I may not, however, be simply equated to the bpy and $423\text{-}DQ^{2+}$ reduction potentials, respectively, for the following reasons. First, placing a second electron in the complex requires not only the energy needed to reduce the ligand, but an additional energy to overcome electron–electron interaction. An estimate of this interaction free energy is provided by the difference in Ru 2+/1+ and Ru 1+/0 potentials in the symmetric, tris complexes $(Ru(bpy)_3^{2+}$, $Ru(DMB)_3^{2+}$, $Ru(TMB)_3^{2+}$, and $[Ru(423\text{-}DQ^{2+})_3]^{8+})$. For these complexes, the first and second electrons each occupy a π^* orbital of the same energy, so the difference in the magnitudes of their Ru 2+/1+ and Ru 1+/0 potentials is attributable to electron–electron interaction alone. For these symmetric complexes, the difference, $E_{1/2}(Ru\ 2+/1+) - E_{1/2}(Ru\ 1+/0)$, is nearly constant, ranging from 180 to 200 mV. Averaging the four values yields an electron–electron interaction free energy, ΔG_{int}, of ca. 185 mV.

Two additional factors preclude simply equating the difference in $E_{1/2}$ values for Ru 1+/0 and Ru 2+/1+ to E_{AR}. First, this difference is a Gibbs free energy, so obtaining an energy from it requires including appropriate entropy terms. Second, again using $Ru(bpy)(423\text{-}DQ^{2+})_2$ as an example, a small, "thermal" effect arises from the fact that the difference in the energies of π^* orbitals localized on the bpy and on the $(423\text{-}DQ^{2+})$ ligands is on the order of one to two kT (kT = 25 mV at room temperature). As a result, some methylated bipyridines of the $423\text{-}DQ^{2+}$ ligands are reduced on the "first" reduction even though it requires more energy. Entropy and thermal effects are considered in detail in Appendix I, where it is shown that E_{AR} for $Ru(bpy)(423\text{-}DQ^{2+})_2$ is related to the Ru 2+/1+ and Ru 1+/0 reduction potentials by the equation:

$$E_{1/2}(Ru(1+/0)) - E_{1/2}(Ru(2+/1+)) - \Delta G_{int} = E_{AR} + E_{AR}K_{eq}\left[\frac{1}{4+K_{eq}} - \frac{2}{1+K_{eq}}\right] - T[\Delta S(Ru(1+/0)) - \Delta S(Ru(2+/1+))]$$

where K_{eq} is defined by eq 4. The "thermal correction" term, involving E_{AR} and K_{eq}, is ca. −20 mV, and the entropy terms yield a small contribution of ca. 5 mV. Whereas $E_{1/2}(Ru(1+/0)) - E_{1/2}(Ru(2+/1+)) - \Delta G_{int}$ is 35 mV, E_{AR} is found to be 50 mV when these terms are included.

It is not possible to determine E_{AR} for $Ru(bpy)_2(423\text{-}DQ^{2+})$ in a manner analogous to the method used for $Ru(bpy)(423\text{-}DQ^{2+})_2$, since the first and second reductions both reduce bpy ligands. Thus the difference in potentials, $E_{1/2}(Ru(1+/0)) - E_{1/2}(Ru(2+/1+))$, 200 mV, is virtually equal to the ΔG_{int} estimate of 185 mV. A simple argument regarding the effects of methyl substitution on ligand reduction potentials, however, leads to the conclusion that E_{AR} in $Ru(bpy)_2(423\text{-}DQ^{2+})$ is the same as that in $Ru(bpy)(423\text{-}DQ^{2+})_2$. In this argument, we suggest that replacing a bpy with a DMB (or $423\text{-}DQ^{2+}$) ligand increases the π^* energy of the other two ligands by the same amount, irrespective of whether they are DMB (or $423\text{-}DQ^{2+}$) or bpy ligands. Replacing a bpy in $Ru(bpy)_2(DMB)^{2+}$ by another DMB (or $423\text{-}DQ^{2+}$) thus increases both the bpy and DMB reduction potentials, with E_{AR} remaining the same. It is therefore concluded that the adjacent–remote MLCT splittings in $Ru(bpy)_2(423\text{-}DQ^{2+})$ and $Ru(bpy)(423\text{-}DQ^{2+})_2$ are, within this assumption, equal. Furthermore, the $Ru(bpy)_2(42n\text{-}DQ^{2+})$ series of complexes (n = 2, 3, 4) are all expected to have the same E_{AR} value, since lengthening the methylene chain linking the diquat's nitrogens is not expected to change ligand π^* energies. This is seen by inspection of Table I, where Ru 2+/1+ and Ru 1+/0 potentials are, respectively, nearly equal for this set of complexes. Thus E_{AR} is determined to be 50 mV for all three complexes.

Evaluation of E_{AR} for $Ru(TMB)_2(423\text{-}DQ^{2+})$ is done in an analogous manner to that done for $Ru(bpy)(423\text{-}DQ^{2+})_2$. Details of this procedure are covered in Appendix I, where a value of −100 mV is obtained for E_{AR}.

In complexes $Ru(DMB)_2(423\text{-}DQ^{2+})$, $Ru(DMB)(423\text{-}DQ^{2+})_2$, and $Ru(423\text{-}DQ^{2+})_3$, E_{AR} values are equal to zero, since DMB and $423\text{-}DQ^{2+}$ ligands have, to a good approximation, the same π^* energies.

Values of E_{AR} are listed in Table III, as are estimates of α, the fraction of MLCT states localized on adjacent ligands, calculated using eq 4 and 5. The table shows that α estimates vary over a wide range, from 6% in $Ru(bpy)_2(423\text{-}DQ^{2+})$ to 96% in $Ru(TMB)_2(423\text{-}DQ^{2+})$. It is the presence of E_{AR}/RT in the exponent of the expression for K_{eq} (eq 4) which is responsible for α's great

(37) Kober, E. M.; Meyer, T. J. *Inorg. Chem.* **1982**, *21*, 3967–3977.

Table IV. Emission Onsets and Maxima for $Ru(bpy)_3^{2+}$ and Related Methyl-Substituted Complexes

complex	λ_{max} (nm)	λ_{onset} (nm)	E_{onset} (eV) $\equiv h\nu$
$(Ru(bpy)_3)^{2+}$	614	556	2.23
$(Ru(bpy)_2DMB)^{2+}$	624	566	2.20
$(Ru(bpy)(DMB)_2)^{2+}$	632	574	2.16
$(Ru(DMB)_3)^{2+}$	625	565	2.19
$(Ru(TMB)_2DMB)^{2+}$	634	571	2.17

sensitivity to changes in the adjacent–remote MLCT splitting.

Variation of k_{et} with Changes in Free Energy. The important role played by α in determining the overall ET rate complicates assessment of a free energy relationship between the log of this rate and the ET driving force (ΔG). Fortunately, this complication is eliminated when considering the $Ru(bpy)_2(42n\text{-}DQ^{2+})$ series of complexes, for $n = 2$, 3, and 4. All three of these compounds have the same MLCT state energies, and therefore the same E_{AR} and α values. As such, they are ideal candidates for assessing the dependence of ET rate on ΔG. This series of complexes differs only in the number of methylene groups in the N–N bridge of their diquat moieties. Lengthening this chain increases the magnitude of (2+/1+) diquat reduction potentials, as indicated in Table I, resulting in a decrease in the driving force for ET to diquat. As n is increased, longer emission decay (forward electron transfer) times are observed (see Table II).

The thermodynamic driving force for ET from MLCT states of a complex to a diquat electron acceptor may be estimated using the following relation:[38]

$$\Delta G = E_{1/2}(\text{Ru } 2+^*/3+) - E_{1/2}(DQ^{2+}(2+/1+)) \quad (6)$$

where the Ru 2+*/3+ potential is a measure of the energy needed to oxidize a complex in an MLCT state. ΔG is related to the difference $E_A - E_B$ indicated in Scheme I. To obtain estimates of Ru 2+*/3+ potentials for the various complexes, Ru 3+/2+ potentials were combined with the energies ($h\nu$) corresponding to the emission onset of the analogous complex not linked to diquat (see Table IV):

$$E_{1/2}(\text{Ru } 2+^*/3+) \cong E_{1/2}(\text{Ru } 3+/2+) - h\nu \quad (7)$$

Several approximations have been used in this approach. First, the energy corresponding to the onset of emission has been used for the lowest MLCT state energy. This onset was determined by extrapolation of the blue edge of the emission spectrum (between 20 and 70% of the emission maximum) to zero intensity. Although this may not result in a completely accurate determination of the energies, it is a reasonable approximation, and previous work has shown that such determinations are consistent with the results of quenching studies.[7] The Franck–Condon factors are likely to be quite similar for all of the complexes studied, and, at worst, this procedure could lead to small systematic shifts in ΔG values. Such shifts are not expected to change the thrust of this discussion. Second, emission onsets have been obtained for compounds analogous to diquat-linked complexes, where DMB ligands replace $42n\text{-}DQ^{2+}$ ligands. This approach was necessary since emission is largely quenched by ET in the $42n\text{-}DQ^{2+}$ complexes. It was shown in the Energetics section that these ligands have the same, or nearly the same, π^* energies, implying that the error incurred in using this procedure is quite small. The third approximation arises from the fact that reduction potentials reflect the Gibbs free energy of a redox process, while photon absorption changes the internal energy of the system. As a result, eq 7 neglects entropy changes on reduction. Solvation entropies are, however, expected to be quite similar in the ground and MLCT states, and entropy changes due to the degeneracy of the MLCT state are at most slightly greater than the Boltzmann constant. Neglect of this term is therefore not expected to introduce serious errors, and it is noted that the same approximation is made in ref 7, where good agreement with quenching studies was obtained.

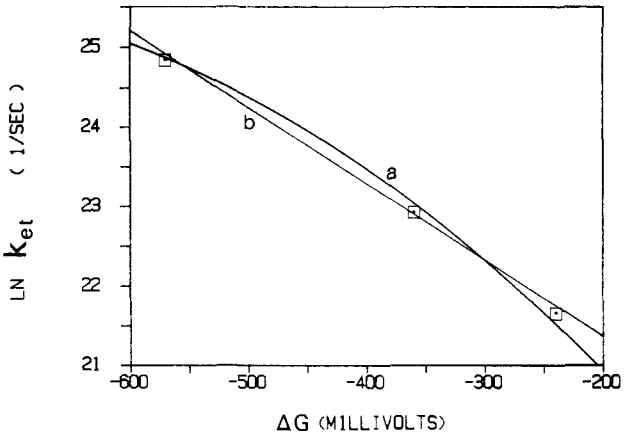

Figure 3. A plot of the log of the adjacent ET rate (k_{et}) versus ET driving force (ΔG) is shown for $Ru(bpy)_2(42n\text{-}DQ^{2+})$, $n = 2$, 3, and 4. Values of k_{et}^{-1} and ΔG are listed in Table III. Curve a is the Marcus theory curve, with $\lambda = 825$ mV, and $A_{et} = 1.4 \times 10^{11}$ (see eq 9 and 10). Curve b is a linear fit to the data (eq 11) with $C = -104$ mV and $b = -2022$ mV.

Since emission occurs from the lowest energy MLCT state, the above described procedure for estimating ΔG is valid provided ET to diquat occurs from this lowest-energy state. This is the case for complexes $Ru(DMB)_2(423\text{-}DQ^{+2})$, $Ru(TMB)_2(423\text{-}DQ^{2+})$, $Ru(DMB)(423\text{-}DQ^{2+})_2$, and $Ru(423\text{-}DQ^{2+})_3$, where the energies of remote MLCT states are greater than or equal to those of adjacent states. For the $Ru(bpy)_2(42n\text{-}DQ^{2+})$ ($n = 2$, 3, 4) and $Ru(bpy)(423\text{-}DQ^{2+})_2$ series of complexes, however, adjacent ligands (like DMB ligands) have higher MLCT state energies. The adjacent–remote MLCT splitting, E_{AR}, must therefore be added to the difference, $E_{1/2}(\text{Ru } 2+^*/3+) - E_{1/2}(DQ^{2+}\ (2+/1+))$, in order to obtain ΔG, yielding the equation:

$$\Delta G = E_{1/2}(\text{Ru } 2+^*/3+) - E_{1/2}(DQ^{2+}(2+/1+)) - E_{AR} \quad (8)$$

Values of ΔG for all the complexes, obtained using eq 6 or 8, are given in Table III, and details of this procedure are covered in Appendix II.

Figure 3 shows a plot of $\ln (k_f(\text{obsd})/\alpha(\text{calcd})) = \ln k_{et}$ vs. ΔG, for the $Ru(bpy)_2(42n\text{-}DQ^{2+})$ ($n = 2$, 3, 4) series of complexes. k_{et}^{-1} values are listed in Table III. In the Energetics section, an E_{AR} value of 50 mV was obtained for these complexes, corresponding to an estimate of α equal to 0.064. This value was used to determine k_{et} from observed values of k_f. Note that even though α is used to determine k_{et}, the *slope* of the $\ln k_{et}$ vs. ΔG plot is independent of it. Any errors in α will thus affect only the intercept.

The observed dependence of ET rate on driving force in the $Ru(bpy)_2(42n\text{-}DQ^{2+})$ ($n = 2$, 3, 4) series of complexes (Figure 3) shows that the rate-limiting step for electron transfer is actually that from the adjacent ligand to diquat, not ET from a remote to an adjacent ligand. (This statement assumes that ET from a remote ligand to diquat is slow, to be discussed later). Ligand-to-ligand electron transfer must therefore occur in less than 250 ps, the fastest decay time for any of the $Ru(bpy)_2(42n\text{-}DQ^{2+})$-type complexes, observed for $Ru(bpy)_2(422\text{-}DQ^{2+})$. Our assumption of fast ligand-to-ligand ET is thus at least partially substantiated by these results.

The activation energy, $\Delta G^{\ddagger}$, for the ET reaction can be related to driving force, ΔG, by the theories of Marcus and Hush for solvent-mediated electron transfer:[35,39-43]

$$\Delta G^{\ddagger} = \frac{\lambda}{4}\left(1 + \frac{\Delta G}{\lambda}\right)^2 \quad (9)$$

(38) Amouyal, E.; Zidler, B.; Keller, P.; Moradpour, A. *Chem. Phys. Lett.* **1980**, *74*, 314–316.

(39) Marcus, R. A. *J. Chem. Phys.* **1965**, *43*, 679–701.
(40) Marcus, R. A. *Annu. Rev. Phys. Chem.* **1964**, *15*, 155.
(41) Marcus, R. A.; Sutin, N. *Inorg. Chem.* **1975**, *14*, 213–216.
(42) Hush, N. *Trans. Faraday Soc.* **1961**, *57*, 557–580.

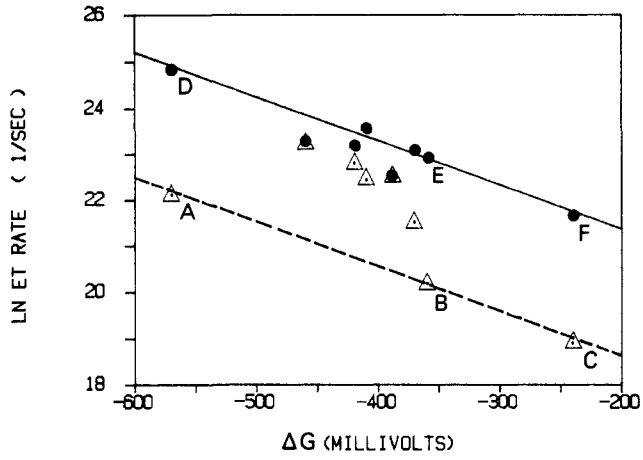

Figure 4. Two plots of the log of the ET rate against driving force (ΔG) are shown. Triangles indicate the plot of ln (k_f(obsd)) vs. ΔG. Points labeled A, B, and C represent Ru(bpy)$_2$(42*n*-DQ^{2+}), for n = 2, 3, and 4, respectively. Note that these points form a line (dotted line). The other triangles, representing the other complexes, do not fall on this line. Solid dots indicate the plot of ln (k_f(obsd)/α(calcd)) vs. ΔG. Points D, E, and F represent Ru(bpy)$_2$(42*n*-DQ^{2+}) (n = 2, 3, and 4, respectively). The solid line is the least-squares fit to these points, shown in Figure 3, and given in eq 11.

where λ is the solvent "reorganization energy". The rate constant, k_{et}, for electron transfer is, in general, given by:

$$k_{et} = A_{et} \exp(-\Delta G^{\ddagger}/RT) \qquad (10)$$

Because of their structural similarities, it is expected that the A_{et} factors will be the same for all the complexes of the Ru(bpy)$_2$-(42*n*-DQ^{2+}) (n = 2, 3, 4) series. The rate of ET is therefore related to ET activation energy and, by eq 9, to ET driving force in Ru(bpy)$_2$(42*n*-DQ^{2+}). Figure 3 shows curve a, corresponding to calculated values of ln (k_{et}) assuming λ = 850 mV, and A_{et} = 1.4 × 10^{11} s^{-1}. This value of λ may be somewhat underestimated since in Ru(bpy)$_2$(422-DQ^{2+}) the electron transfer rate may be partially limited by the rate of ligand-to-ligand ET.

The data in Figure 3 may also be fit (curve b) with a simpler linear free energy relationship:

$$C \ln k_{et} = \Delta G + b \qquad (11)$$

where C and b are constants. Emission quenching rates for the Ru(bpy)$_2$(42*n*-DQ^{2+}) series of complexes may be used to evaluate C and b. Least-squares fitting yields C = −104 mV and b = −2022 mV, with α equal to 0.064. With values of C and b in hand, eq 11 and the ΔG values given in Table III may be used to estimate k_{et} in the other complexes, where MLCT state energies vary from those in the Ru(bpy)$_2$(42*n*-DQ^{2+}) series. Such estimates of k_{et}^{-1} are listed in Table III, and the details of determination of k_{et} are given in Appendix II.

Validity of Proposed Model. Figure 4 summarizes the role of adjacent MLCT state population in determining the overall ET rate (k_f). In this figure, the log of the observed ET rate (ln k_f) (triangles) and ln (k_f/α) (solid dots) are plotted against driving force (ΔG). In the ln k_f vs. ΔG plot, points (A, B, and C, respectively) corresponding to Ru(bpy)$_2$(42*n*-DQ^{2+}) (n = 2, 3, 4) form a straight line (dotted line). This line has the same slope as the least-squares line shown in Figure 3; it is merely shifted up by −ln α (α = 0.064). Note, however, that points corresponding to other complexes do not fall on this line. Alternatively, the plot of ln (k_f/α)vs ΔG (solid dots) is reasonably linear for all the complexes. The solid line shown is the least-squares line shown in Figure 3. Dividing k_f by α has the effect of raising each of the points represented by triangles by an amount equal to −ln α. In particular, the positions of the points representing the Ru-(bpy)$_2$(42*n*-DQ^{2+}) series (A, B, and C, respectively) change dramatically (to D, E, and F, respectively), owing to the small value of α. As a result, points representing the Ru(bpy)$_2$(42*n*-DQ^{2+}) series, in the ln k_f/α vs. ΔG plot, line up reasonably well with the other solid dots, representing the other complexes.

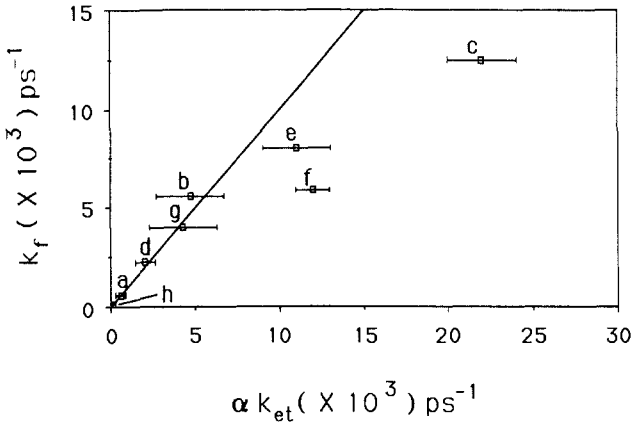

Figure 5. Estimates of αk_{et} are plotted against observed k_f values. A 45° line is shown; points falling on or near this line (αk_{et} = k_f) indicate success of the model. Points are labeled as follows: (a) Ru(bpy)$_2$(423-DQ^{2+}), (b) Ru(DMB)$_2$(423-DQ^{2+}), (c) Ru(TMB)$_2$(423-DQ^{2+}), (d) Ru(bpy)$_2$(423-DQ^{2+}), (e) Ru(DMB)(423-DQ^{2+})$_2$, (f) Ru(423-DQ^{2+})$_3$, (g) Ru(bpy)$_2$(422-DQ^{2+}), (h) Ru(bpy)$_2$(424-DQ^{2+}).

Figure 4 clearly shows that the small value of α accounts for the long decay time observed for Ru(bpy)$_2$(423-DQ^{2+}) relative to that observed for the other 423-DQ^{2+}-type complexes. This observation is strong evidence for success of the model, since the order of magnitude difference in rates between Ru(bpy)$_2$(423-DQ^{2+}) and, for example, Ru(DMB)$_2$(423-DQ^{2+}) is the most striking feature of the kinetic data. As shown in the next section, the 15% difference in driving force estimates for these two complexes would account for just a factor of 1.6 slower rate for Ru(bpy)$_2$(423-DQ^{2+}); it is only when the small value of α is considered that the order of magnitude difference in rates is explained.

In Figure 5, k_f(obsd) is plotted against the product of α(calcd) and k_{et}(calcd), where α, k_{et}^{-1}, and $(\alpha k_{et})^{-1}$ are given in Table III. Error bars in Figure 5 reflect the uncertainty in α and in ET driving force arising from ±10-mV uncertainties in E_{AR} and ΔG estimates. A linear plot with a slope of unity (αk_{et} = k_f) indicates success of the model. With the exceptions of Ru(TMB)$_2$(423-DQ^{2+}) and Ru(423-DQ^{2+})$_3$, the points, within estimated errors, lie on or very close to the 45° line. In particular, for complexes Ru(DMB)$_2$(423-DQ^{2+}) and Ru(DMB)(423-DQ^{2+})$_2$, the model predicts values of $(\alpha k_{et})^{-1}$ (212 and 94 ps, respectively) which are close to those actually observed (180 and 125 ps, respectively). It also predicts Ru(TMB)$_2$(423-DQ^{2+}) to have the fastest decay time (45 ps). This complex is indeed observed to have the fastest decay time (80 ps), though it is twice as long as the estimate. For Ru(bpy)(423-DQ^{2+})$_2$ the observed value of k_f^{-1} is 450 ps, in excellent agreement with the $(\alpha k_{et})^{-1}$ estimate (490 ± 145 ps) shown in Table III. A decay time of 85 ps is predicted for Ru(423-DQ^{2+})$_3$, where 170 ps is measured. We believe that the Ru(423-DQ^{2+})$_3$ complex is a special case, and will consider it later in this section.

For the complexes Ru(DMB)$_2$(423-DQ^{2+}) and Ru(DMB)-(423-DQ^{2+})$_2$, the three ligand π^* levels are nearly isoenergetic. No subsequent calculation from measured values of Ru 2+/1+ and Ru 1+/0 reduction potentials in Ru(DMB)$_3^{2+}$ or Ru(423-DQ^{2+})$_3$ is needed to estimate an E_{AR} value of zero. It is therefore expected that estimates of α for these complexes would be quite accurate. As stated earlier, calculation of α is very sensitive to variations in E_{AR}, the adjacent–remote MLCT gap. The agreement between observed values of k_f and calculated values of αk_{et} undoubtedly depend in part on how well the energy gaps, ΔG, and especially E_{AR}, are known.

In the case of Ru(TMB)$_2$(423-DQ^{2+}), even though an involved procedure was used to determine E_{AR}, its magnitude is so large (E_{AR} = −100 mV) that errors of even 20 mV will not change α by more than 10%.

(43) Reynolds, W. L.; Lumry, R. W. *Mechanisms of Electron Transfer*; Ronald Press: New York, 1966; Chapter 6.

Uncertainties in E_{AR} are likely to have the most severe effects on estimates of α for the complexes Ru(bpy)$_2$(42n-DQ^{2+}) and Ru(bpy)(423-DQ^{2+})$_2$. In these cases, once again a fairly involved procedure was used to determine E_{AR}. If our estimate of E_{AR} were too small, α would be too large, and vice versa. A low estimate of α in Ru(bpy)$_2$(42n-DQ^{2+}) would result in a more negative estimate of the intercept, b, in eq 11. Such an error would cause estimates of k_f for the other complexes to be too large. An error in the E_{AR} estimate for Ru(bpy)$_2$(423-DQ^{2+}) might thus be detected as a systematic shift in expected decay times in relation to those observed for all of the other complexes. This does not appear to be the case. In particular, the reasonable agreement between observed and estimated k_f^{-1} values for the complexes Ru(DMB)$_2$(423-DQ^{2+}) and Ru(DMB)(423-DQ^{2+})$_2$ supports the 50-mV estimate of E_{AR} in Ru(bpy)$_2$(423-DQ^{2+}), and we are therefore satisfied with this value.

As stated earlier, Ru(423-DQ^{2+})$_3$ is believed to be a special case. In this complex, each ligand has a +2 charge. Repulsion of the charged ligands could lead to an increased ligand-to-diquat ET distance. Our simple scheme does not account for variations in this parameter. If the ET distance were indeed longer in Ru(423-DQ^{2+})$_3$, the calculated value of the ET time, $(\alpha k_{et})^{-1}$, is expected to be too short. Even given this caveat, the deviation of the predicted value from the experimental value of k_f^{-1} is only a factor of 2. For these reasons, we are therefore not too troubled by the short predicted decay time in this complex.

Discussion of Assumptions. In general, the proposed model leads to semiquantitative agreement with observed ET times. The two major assumptions leading to this model will now be considered, namely, that (1) ET from remote ligands to the diquat is slow and therefore not important, and (2) ligand to ligand electron hopping is fast relative to ligand-to-diquat ET. Let us assume that remote and adjacent ET rates are similar and consider the consequences. In the case of Ru(bpy)$_2$(423-DQ^{2+}), the small value of α would no longer explain the long ET time in this complex, since ET from remote ligands would occur at a similar rate. In this case, the difference in measured ET rates between this complex and Ru(DMB)$_2$(423-DQ^{2+}), for instance, would be due only to variations in π^* energy, leading to variations in ΔG. Using eq 11 and the values of ΔG from Table III, it is found that such variation would be responsible for only a factor of 1.6 faster rate for the latter complex. The observed difference is nearly a factor of 10, ruling out similar adjacent and remote ET rates.

Further evidence for the likelihood of slow ET from remote bipyridines to the diquat is provided by additional kinetic data obtained for the related complex Ru(bpy)$_2$(453-DQ^{2+}). The only difference between this complex and Ru(bpy)$_2$(423-DQ^{2+}) is the longer length, five units, of the methylene chain linking bipyridine to diquat. Space-filling molecular models, assuming an extended configuration, show that the adjacent ET distance in Ru(bpy)$_2$(453-DQ^{2+}) is longer than the adjacent ET distance in Ru(bpy)$_2$(423-DQ^{2+}), but shorter than the remote distance in the latter complex. We have measured the emission decay time in Ru(bpy)$_2$(453-DQ^{2+}) to be on the order of 30 ns, much longer than that for Ru(bpy)$_2$(423-DQ^{2+}). It may be concluded from these observations that, in general, the longer remote ET distance is likely to cause ET from remote ligands to diquat to be much slower than that from an adjacent ligand.

Although the above arguments show that remote ET is probably slow, it is not possible to rule it out completely. This is especially true in complexes where a large fraction of the population is on a remote ligand. Without direct evidence of remote to diquat ET, we can only say that its rate is much slower than that from adjacent, and that ignoring it yields reasonable agreement with experiment.

Now consider the second assumption, that ligand-to-ligand ET is fast. As stated earlier, initial excitation (355 nm) is largely into metal-centered d–d states, with some absorption into π–π^* (bpy) states. This is followed by decay to emissive ^{3}MLCT states.[44] If it is assumed that these ^{3}MLCT states are equally populated after energy relaxation, then the initial fraction of adjacent MLCT state population will simply be $n_A/3$. If ET from ligand to ligand were much slower than that from adjacent ligand to diquat, biphasic behavior would be expected for both emission decay and bleach recovery kinetics. One component, of relative intensity $n_A/3$, would have a decay time equal to the adjacent ET time. The other would have relative intensity $n_R/3$, and a decay time equal to either the ligand-to-ligand ET time, or the remote ET time. Since single exponential behavior was observed for all the complexes, it is concluded that ligand-to-ligand ET cannot be slower than adjacent ET. Furthermore, it has already been mentioned that for all the complexes studied, a free energy relationship was found to exist between ET rate and ET driving force, also suggesting that the slow step is indeed ET to diquat, not from ligand to ligand.

To put limits on the ligand-to-ligand ET rate, consider the example of Ru(TMB)$_2$(423-DQ^{2+}). In this complex, the equilibrium population of the adjacent MLCT state is 96%, implying that the remote population will decrease from its initial value of 0.67 upon excitation, to 0.04 at equilibrium. The ligand-to-ligand ET time must therefore be shorter than the apparent ET time (80 ps), since ET from ligand to ligand is required for the transfer of electrons to diquat to be complete. The 45-ps predicted decay time is about a factor of 2 faster than that observed, resulting in significant deviation from the 45° line in Figure 5. Although there is no direct experimental evidence of it, a breakdown of the fast ligand-to-ligand ET assumption could be responsible for this deviation. It must be emphasized, however, that whether or not ligand-to-ligand ET is rate limiting in this case, the observed 80-ps decay time may still be used as a limiting value for this process in Ru(TMB)$_2$(423-DQ^{2+}).

Ligand-to-ligand ET may occur at a faster rate in Ru(TMB)$_2$(423-DQ^{2+}) than it does in the other complexes, since its driving force (−100 mV) is greatest. The complexes with the longest remote-to-adjacent ligand ET times are probably the Ru(bpy)$_2$(42n-DQ^{2+}), n = 2, 3, 4 series, where adjacent MLCT states are 50 mV higher in energy than remote. However, even in these possibly slowest cases, ligand-to-ligand ET occurs in less than 250 ps, the observed ET time for Ru(bpy)$_2$(422-DQ^{2+}).

Ligand-to-ligand electron transfer may actually be much faster than these upper limit estimates. To estimate a lower limit, we note that excited-state time-resolved resonance Raman spectra of Ru(bpy)$_3^{2+}$ and related complexes have line widths of a few wavenumbers.[14,15] These lines are due to scattering from MLCT states, where an electron is localized on a single ligand, and the line widths thus correspond to a lower limit for electron hopping on the order of a few picoseconds.

No direct measurement of ligand-to-ligand ET rates in liquid solutions appear to have been made, although it is clear from this discussion that such values are needed. Time-resolved studies to directly measure ligand-to-ligand ET rates and their temperature dependences are currently in progress.

V. Conclusions

It has been shown that the rate of ET from MLCT states of methyl-substituted ruthenium tris(bipyridine) to linked diquat acceptors may be understood in terms of energetics and a simple kinetic model. The model assumes fast ligand-to-ligand ET, allowing an equilibrium to be established between adjacent and remote MLCT state populations, and relatively slow ET from remote MLCT states to the diquat acceptor. Differences in ET rates for the complexes studied have been found to be due largely to variations in α, the fraction of MLCT states localized on ligands adjacent to diquat electron acceptors. Breakdown of the model may occur when forward ET is very fast. It has also been shown that reverse ET, repopulating the ground state, is much faster than forward, for all complexes studied. In addition, a free energy relationship between the ET rate and ET driving force has been established.

Acknowledgment. This work was supported by the National Science Foundation (C. M. Elliott/Grant CHE-8516904 and D.

(44) Belser, P.; Von Zelewsky, A.; Juris, A.; Barigelletti, F.; Balzani, V. *Chem. Phys. Lett.* **1984**, *104*, 100–104.

F. Kelley/Grant CHE-8517528).

Appendix I. Determination of E_{AR}

To determine the energy difference between MLCT states localized on adjacent and remote ligands, E_{AR}, reduction potentials need to be related to the energies E_A and E_R (see Scheme I). The Ru (2+/1+) potential corresponds to the free energy of a singly reduced complex at room temperature. Relating this quantity to the average value of the energy of a singly reduced system requires inclusion of a term equal to the entropy change ($T\Delta S$) on Ru (2+/1+) reduction. With this term included, the following expression may be written for the average energy of singly reduced systems, E_{SR}:

$$E_{SR} = E_{1/2}(\mathrm{Ru}(2+/1+)) + T\Delta S(\mathrm{Ru}(2+/1+)) = p_A E_A + p_R E_R \quad (A1)$$

where p_A and p_R are the probabilities associated with occupation of the states with energies E_A and E_R, respectively, and are given by:

$$p_A = (n_A/n_R)f/[(n_A/n_R)f + 1] = K_{eq}/(1 + K_{eq}) \quad (A2a)$$

$$p_R = 1/[(n_A/n_R)f + 1] = 1/(1 + K_{eq}) \quad (A2b)$$

The quantity f is equal to $\exp(-E_{AR}/RT)$, and n_A and n_R are the respective numbers of adjacent and remote ligands. K_{eq} was defined previously and is equal to $(n_A/n_R)\exp(-E_{AR}/RT)$. In writing eq A1, we have used the fact that $E_{1/2}$ values are free energies, and the relation $G = E - TS$ (no pV work). $E_{1/2}$, $T\Delta S$, and E_{SR} are assumed to have the same units, and whenever $E_{1/2}$ appears, this is taken to mean $|E_{1/2}|$.

Combining eq A2 and A2 gives

$$E_{SR} = E_R + (n_A/n_R)fE_{AF}/[(n_A/n_R)f + 1] = E_R + K_{eq}E_{AR}/(1 + K_{eq}) \quad (A3)$$

This relation is general, true for $n_A = 2$, $n_R = 1$ and for $n_A = 1$, $n_R = 2$.

In order to calculate $\Delta S(\mathrm{Ru}(2+/1+))$, the relation,

$$-S/R = \sum_j p_j \ln p_j \quad (A4)$$

is used. This yields the expression:

$$\frac{\Delta S}{R}(\mathrm{Ru}(2+/1+)) = \ln(1 + (n_A/n_R)f) - \frac{(n_A f/n_R)\ln(n_A f/n_R)}{1 + (n_A f/n_R)} = \ln(1 + K_{eq}) - (K_{eq}\ln K_{eq})/(1 + K_{eq}) \quad (A5)$$

which, again, is a general result.

For doubly reduced systems, $E_{1/2}(\mathrm{Ru}(1+/0))$ is a measure of the additional free energy required to reduce a second ligand in the complex, once the first ligand is already reduced. Thus the sum $E_{1/2}(\mathrm{Ru}(1+/0)) + E_{1/2}(\mathrm{Ru}(2+/1+))$ corresponds to the free energy of a doubly reduced complex. Once again, in order to write this quantity in terms of energies, $T\Delta S$ terms must be included, and the average energy of the doubly reduced complex, E_{DR}, is given by:

$$E_{DR} = E_{1/2}(\mathrm{Ru}(1+/0)) + E_{1/2}(\mathrm{Ru}(2+/1+) + T\Delta S(\mathrm{Ru}(1+/0)) + T\Delta S(\mathrm{Ru}(2+/1+)) - \Delta G_{int} \quad (A6)$$

ΔG_{int}, as was defined in the Energetics section, is the electron–electron interaction free energy. Subtracting it from the sum in eq A6 allows the result to be viewed as the average value of the energy of a doubly reduced, noninteracting system.

E_{DR} depends on the number of adjacent and remote ligands in the complex. If we define E_1 and E_2 to be the first and second energy levels of the system where $n_A = 2$ and $n_R = 1$, then

$$E_1 = E_A + E_R$$

and

$$E_2 = 2E_A$$

The probabilities, p_1 and p_2, corresponding to states with these energies are given by

$$p_1 = 1/[1 + (n_R f/n_A)] \quad (A7a)$$

$$p_2 = (n_R f/n_A)/[1 + (n_R f/n_A)] \quad (A7b)$$

The average value of the energy of this doubly reduced system, E_{DR} ($n_A = 2$, $n_R = 1$), is thus given by:

$$E_{DR}(n_A{=}2,n_R{=}1) = E_A + E_R + \frac{(n_R f/n_A)E_{AR}}{1 + (n_R f/n_A)} = E_A + E_R + \frac{fE_{AR}}{2 + f} \quad (A8)$$

Using eq A4 once again, $\Delta S(R_u(1+/0))/R$ is found to be:

$$\frac{\Delta S}{R}(\mathrm{Ru}(1+/0)) = \ln(1 + (n_R f/n_A)) - \frac{(n_R f/n_A)\ln(n_R f/n_A)}{1 + (n_R f/n_A)} \quad (A9)$$

For the $n_A = 1$, $n_R = 2$ case, state energies (called E_1' and E_2') are given by:

$$E_1' = 2E_R \qquad E_2' = E_A + E_R \quad (A10)$$

with corresponding probabilities, p_1' and p_2', respectively equal to p_1 and p_2 (see eq A7a and A7b, with the value of $n_A = 1$ and $n_R = 2$). Using eq A7 and A10 yields the equation:

$$E_{DR}(n_A{=}1,n_R{=}2) = 2E_R + \frac{E_{AR}(n_R f/n_A)}{1 + (n_R f/n_A)} = 2E_R + \frac{2E_{AR}f}{(1 + 2f)} \quad (A11)$$

The complex Ru(bpy)(423-DQ^{2+})$_2$ has $n_A = 2$ and $n_R = 1$. If eq A1, A3, A5, A6, A8 and A9 are combined, the resulting equation has just one unknown, E_{AR}:

$$E_{1/2}(\mathrm{Ru}(1+/0)) - E_{1/2}(\mathrm{Ru}(2+/1+)) - \Delta G_{int} = E_{DR}(n_A{=}2,n_R{=}1) - 2E_{SR} + T[\Delta S(\mathrm{Ru}(2+/1+) - \Delta S(\mathrm{Ru}(1+/0)] = E_{AR} + E_{AR}f[1/(2 + f) - 4/(1 + 2f)] + RT[\ln(1+ 2f) - (2f\ln(2f))/(1 + 2f) - \ln(1 + f/2) + (f/2)\ln(f/2)/(1 + f/2)] \quad (A12)$$

This self-consistent equation leads to a value of 50 mV for E_{AR} in Ru(bpy)(423-DQ^{2+})$_2$. The entropy term is ca. 5 mV, and the term involving E_{AR} and f, the "thermal correction", is ca. 20 mV.

In cases where $n_A = 1$ and $n_R = 2$, combination of eq A1, A3, A5, A6, A9, and A11 yields

$$E_{1/2}(\mathrm{Ru}(2+/1+)) - E_{1/2}(\mathrm{Ru}(1+/0)) - \Delta G_{int} = E_{DR}(n_A{=}1,n_R{=}2) - 2E_{SR} - T[\Delta S(\mathrm{Ru}(2+/1+)) - \Delta S(\mathrm{Ru}(1+/0))] = E_{AR}(2f)[1/(1 + 2f) - 1/(2 + f)] + RT[\ln(1 + f/2) - (f/2)\ln(f/2)/(1 + f/2) - \ln(1 + 2f) + (2f)\ln(2f)/(1 + 2f)] \quad (A13)$$

This expression is used to solve for E_{AR} for the complex Ru(TMB)$_2$(423-DQ^{2+}), yielding a value of −100 mV. The entropy term is quite small, less than 3 mV in magnitude.

Appendix II. Numerical Determination of ΔG, k_{et}^{-1}, and $(\alpha k_{et})^{-1}$

The method for determination of E_{AR} and α for all the complexes is described in the Energetics section in Appendix I. These values are listed in Table III.

In order to estimate the adjacent ET rate, k_{et}, for all the complexes, the ET driving force, ΔG, must be determined. This is done in a two-step process. First, an estimate of the Ru 2+*/3+ potential is made using eq 7. The Ru 3+/2+ potential in this equation is given in Table I, and $h\nu$ is taken to be the onset of emission for the appropriate complex in Table IV. Once an estimate of Ru 2+*/3+ is made, eq 6 or 8 is used to evaluate ΔG. These equations ignore the small thermal and entropy effects discussed in Appendix I. Such effects are expected to be negligible here, since values of ΔG are large in magnitude (−240 to −600 mV). Equation 8 is used for complexes Ru(bpy)$_2$(42n-DQ^{2+}) (n = 2, 3, and 4), and Ru(bpy)(423-DQ^{2+})$_2$, where the adjacent

MLCT state is higher in energy than remote. For all other complexes eq 6 is employed. For all 423-type complexes, the DQ^{2+} 2+/1+ reduction potential is -0.65 V, as shown in Table I. Once values of ΔG are known, estimation of k_{et} follows easily, using eq 11, with $C = -104$ mV, and $b = -2022$ mV. Estimates presented in this Appendix are listed in Table III.

$(Ru(bpy)_2(42n\text{-}DQ^{2+}))^{4+}$ Series. The onset of emission in the complex $Ru(bpy)_2(DMB)^{2+}$ is 2.20 eV (Table IV), and the Ru 3+/2+ potential for $Ru(bpy)_2(423\text{-}DQ^{2+})$ is +1.24 V (Table I). Equation 7 thus yields a value of 1.24 - 2.20 = -0.96 V for the Ru 2+*/3+ potential in $Ru(bpy)_2(423\text{-}DQ^{2+})$. With values of -0.65 V for the DQ^{2+} 2+/1+ potential, and 0.05 V (50 mV) for E_{AR}, eq 8 yields an estimate of ΔG equal to -0.96 + 0.65 - 0.05 = -0.36 V or -360 mV. For $Ru(bpy)_2(422\text{-}DQ^{2+})$ and $Ru(bpy)_2(424\text{-}DQ^{2+})$, DQ^{2+} 2+/1+ potentials (Table I) are -0.44 and -0.77 V, respectively, yielding respective ΔG estimates (Table III) of -240 and -570 mV. For these complexes, k_{et} values are estimated as $k_f(obsd)/\alpha(calcd)$, ($\alpha = 0.064$). These k_{et}^{-1} estimates are found in Table III.

$(Ru(DMB)_2(423\text{-}DQ^{2+}))^{4+}$. The onset of emission in the complex $Ru(DMB)_3^{2+}$ (2.19 eV, Table IV) and the Ru 3+/2+ potential (+1.13 V, Table I) are combined using eq 7, to yield a value of 1.13 - 2.19 = -1.06 V for the Ru 2+*/3+ potential. With the DQ^{2+} 2+/1+ potential equal to -0.65 V, eq 6 yields an estimate for ΔG equal to -1.06 + 0.65 = -0.41 V or -410 mV. Finally, k_{et} is determined from ΔG using eq 11, yielding a value of 1.4×10^{-2} ps^{-1} (k_{et}^{-1} is thus 70 ps). Since E_{AR} is zero, eq 4 and 5 yield a value of α of 0.33 (Table III). Combining α and k_{et} results in a value of 212 ps for $(\alpha k_{et})^{-1}$.

$(Ru(TMB)_2(423\text{-}DQ^{2+}))^{4+}$. The onset of emission in the complex $Ru(TMB)_2(DMB)^{2+}$ (2.17 eV, Table IV) and the Ru 3+/2+ potential (+1.06 V, Table I) are substituted into eq 7, yielding a value of 1.06 - 2.17 = -1.11 V for the Ru 2+*/3+ potential. For this complex, the adjacent MLCT energy is lower than that of remote, so eq 6 is used to find ΔG. This yields a value of -1.11 + 0.65 = -0.46 V, or -460 mV, for ΔG. Equation 11 then yields an estimate of k_{et} equal to 2.31×10 10^{-2} ps^{-1} (k_{et}^{-1} = 43 ps). Equations 4 and 5, with $E_{AR} = -100$ mV, yield a value of 0.96 for α (Table III). Combining this quantity with k_{et}^{-1}, $(\alpha k_{et})^{-1}$ is estimated to be 45 ps.

$(Ru(bpy)(423\text{-}DQ^{2+})_2)^{6+}$. The emission onset in $Ru(bpy)(DMB)_2^{2+}$ (2.16 eV, Table IV) and the Ru 3+/2+ potential (+1.19 V, Table I) are combined using eq 7 to give a value of 1.19 - 2.16 = -0.97 V for the Ru 2+*/3+ potential. Equation 8 is employed to estimate ΔG in this complex, since the adjacent MLCT energy is greater than remote. E_{AR} was found to be 0.05 V, and the DQ^{2+} (2+/1+) potential is -0.65 V. Equation 8 thus yields a value of ΔG equal to -0.97 + 0.65 - 0.05 = -0.37 V or -370 mV. Equation 11 then yields an estimate of k_{et} of 9.7×10^{-3} ps^{-1}, and k_{et}^{-1} is thus 103 ps. Equations 4 and 5, with E_{AR} = 50 mV, yield an α value of 0.21 (Table III). $(\alpha k_{et})^{-1}$ is thus estimated to be 490 ps.

$(Ru(bpy)(423\text{-}DQ^{2+})_2)^{6+}$. To estimate the Ru 2+*/3+ potential, the onset of emission in $Ru(DMB)_3^{2+}$ (2.19 eV, Table IV) and the Ru 3+/2+ reduction potential (+1.12 V, Table I) are combined using eq 7 to yield a value of 1.12 - 2.19 = -1.07 V. Equation 6 is employed for estimation of ΔG, with a DQ^{2+} (2+/1+) potential of -0.65 V. Thus ΔG is equal to -1.07 + 0.65 = -0.42 V, or -420 mV. Equation 11 yields a k_{et} estimate of 1.6 $\times 10^{-2}$ ps^{-1}, and k_{et}^{-1} is thus 63 ps. Equations 4 and 5, with E_{AR} = 50 mV, yield an α value of 0.67 (Table III), so $(\alpha k_{et})^{-1}$ is thus found to be 94 ps.

$(Ru(423\text{-}DQ^{2+})_3)^{8+}$. For this complex, there is a diquat electron acceptor on each ligand, so α is equal to unity. Using the emission onset in $Ru(DMB)_3^{2+}$ (2.19 eV) and the Ru 3+/2+ reduction potential of +1.15 V (Table I), the Ru 2+*/3+ potential is calculated to be -1.04 V. With the DQ^{2+} 2+/1+ reduction potential equal to -0.65, eq 6 yields a value of ΔG of -1.04 + 0.65 = -0.39 V, or -390 mV. k_{et}^{-1} is thus 85 ps. Since α is 1.0, k_f^{-1} is 85 ps, as well.

Appearance Potentials of $C_nH_{2n+2}N^+$ Ions (n = 1-3)

S. W. Sigsworth, R. G. Keesee, and A. W. Castleman, Jr.*

Contribution from the Department of Chemistry, The Pennsylvania State University, University Park, Pennsylvania 16802. *Received December 24, 1987*

Abstract: Considerable discrepancy exists in the literature over the appearance potentials for $C_nH_{2n+2}N^+$ ions arising from mono-, di-, and trimethylamine. Through observation of the reactions of the parent molecules with selected metal ions in a flow tube apparatus, both upper and lower limits are determined for the appearance potentials. For $AP(C_2H_6N^+)$ and $AP(C_3H_8N^+)$, 9.9 ± 0.1 eV is the upper limit and 9.2 ± 0.2 eV is the lower limit, while for CH_4N^+ the values are 9.9 ± 0.1 ≤ $AP(CH_4N^+)$ ≤ 10.6 ± 0.1 eV.

A number of values have been reported for the appearance potentials of certain $C_nH_{2n+2}N^+$ ions formed from amines. For example, in the case of the appearance of $C_2H_6N^+$ [$AP(C_2H_6N^+)$] from dimethylamine, the values range from 9.41 ± 0.06 to 10.50 eV.[1-3] Through new studies reported herein, we are able to provide both lower and upper limits for the appearance potentials of $C_2H_6N^+$ as well as CH_4N^+ and $C_3H_8N^+$ formed from mono-, di-, and trimethylamine (MMA, DMA, and TMA), respectively. The limiting values are derived from measurements of reactions of the parent molecules with selected metal ions.

Investigations[4] of the product distributions and mechanisms for the reaction of cobalt ion with a number of primary, secondary, and tertiary amines showed that, in each case, α-hydride abstraction to form neutral CoH and the $C_nH_{2n+2}N^+$ ion from the amine is a substantial, if not the major, reaction pathway. By analogy, recent studies in our laboratory of reactions of copper and silver ions are also consistent with an α-hydride abstraction mechanism for both DMA and TMA (also for MMA with copper ion), and we have been able to utilize these findings to determine the requisite appearance potentials as discussed in what follows.

(1) Solka, B. H.; Russell, M. E. *J. Phys. Chem.* **1974**, *78*, 1268.
(2) Loudon A. G.; Webb, K. S. *Org. Mass Spectrom.* **1977**, *12*, 283.
(3) Taft, R. W.; Martin, R. H.; Lampe, F. W. *J. Am. Chem. Soc.* **1965**, *87*, 2490.
(4) Radecki, B. D.; Allison, J. *J. Am. Chem. Soc.* **1984**, *106*, 946.

0002-7863/88/1510-6682$01.50/0